Revista Brasileira de Física Tecnológica Aplicada, v.3,n.1, junho de 2016.

Spectroscopic study of Nafion® membrane as a function of water content by Phase-Resolved Photoacoustic Method

Estudo espectroscópico de membrana Nafion® em função do teor de água usando o Método de Separação de Espectros na Fase

Estudio espectroscópico de la membrana Nafion® como una función del contenido de agua mediante los espectros en el Método de Separación de Fases

[1]Guy Lopes, Daniele Toniolo Dias, Juliana Soares de Souza, Caroline Dias Rosa

Abstract: Nafion® membranes were developed by DuPont, a perfluorosulfonic acid/polytetrafluoroethylene copolymer. These membranes are hydrophilic and the water is preferentially sorbed into the clusters due to the hydrophobic character of fluorocarbon matrix. The sulfonic acid groups are chemically active and fixed within the Teflon polymer matrix. Thus, this first synthetic ionic polymer is chemically resistant and durable, making it useful for Proton Exchange Membrane fuel cells. In order to monitoring the groups -OH of the Nafion®, we used the Photoacoustic Spectroscopy phases. The optical absorption spectrum was determined for wavelengths of 800 to 2600 nm. The procedure was to measure the samples in different hydration times. Using the Phase-Resolved Photoacoustic method, it was possible to separate the contribution of –OH, of C=O and of methylene group. The phase lag as a water function behaviors found may be associated with structural changes induced by membrane hydration.

Keywords: fuel cell; hydration; photoacoustic

Resumo: Membranas de Nafion® são filmes desenvolvidos pela DuPont, um copolímero ácido perfluorosulfônico/politetrafluoroetileno. Estas membranas são hidrofílicas e a água é preferencialmente absorvida para os clusters devido ao caráter hidrofóbico da matriz de fluoro carbônica. Os grupos ácidos sulfônico são quimicamente ativos e fixos dentro da matriz do polímero Teflon. Assim, este primeiro polímero iônico sintético é quimicamente resistente e durável, tornando-o útil para células combustíveis a membrana trocadora de prótons. A fim de monitorar os grupos -OH da membrana Nafion®, usamos as fases da Espectroscopia Fotoacústica. O espectro de absorção óptica foi determinado para comprimentos de onda de 800 a 2600 nm. O procedimento foi analisar as amostras em diferentes tempos de hidratação. Utilizando o Método de Separação de Espectros na Fase, foi possível separar a contribuição de -OH, de C = O e de grupo metileno. Os comportamentos da diferença de fase em função da hidratação encontrados podem estar associados com alterações estruturais induzidas pela hidratação da membrana.

Palavras-chave: célula combustível; hidratação; fotoacústica

Resumen: Membranas Nafion® son películas desarrolladas por DuPont, un copolímero ácido perfluorosulfónico/politetrafluoroetileno. Esas membranas son hidrofílicas y, el agua, preferencialmente, se absorbe para los clusters, debido al carácter hidrofóbico de la matriz de fluoro carbónica. Los grupos ácidos sulfónicos son químicamente activos y fijos dentro de la matriz de polímero de Teflón. Así que, este primer polímero iónico sintético es químicamente resistente y durable, lo que lo vuelve útil para células combustibles a membrana intercambiadora de protones. Con el fin de monitorizar los grupos -OH de la membrana Nafion®, hemos utilizado las fases de Espectroscopía Fotoacústica. Se determinó el espectro de absorción óptica para longitudes de ondas de 800 a 2600 nm. Se evaluó las muestras a diferentes tiempos de hidratación. Utilizando el Método de Separación Espectral en la Fase, ha sido posible separar la contribución de -OH, C=O y de grupo metileno. Los comportamientos de la diferencia de fase en función de la hidratación encontrados pueden estar relacionados a cambios estructurales inducidos por la hidratación de la membrana.

Palabras clave: pilas de combustible; hidratación; fotoacústica

[1] Master's Degree student in the PPGEM at Federal University of Technology – Paraná, Ponta Grossa, email: guy_lopes@hotmail.com

1. Introduction

There is great scope for new alternatives for power generation due to reduction of current energy reserves and the increased energy demand. The fuel cells (FC), even considering they are an old technology, received great attention because of theirs high energy efficiency and low emissions of the waste via incineration. Considered "energy sources of the future" the most promising FC for applications in mobile and portable devices is the PEM (Proton Exchange Membrane) whose research is focused mainly on the polymeric membranes development, to cut production costs.

Among the classes of polymers, the most promising as a PEM is the Nafion® based on their physicochemical properties and it's perfluorinated ionomers (PERLES, 2008). Considered the most efficient electrolyte in fuel cells, Nafion® is a tetrafluoroethylene based on fluorine polymer-copolymer discovered in the late 60s by Walther Grot of DuPont, and is in the first class of synthetic polymers with ionic properties, which are called ionomer.

The unique properties of Nafion® are a result of the incorporation of perflorovinil group of the ethers with sulfonate group terminated with tetrafluoroethylene (Teflon) as a base (CHURCH, 2006).

The Nafion® is a polymer that has hydrophilic and hydrophobic domains, where in the main chain, whose composition is similar to Polytetrafluoroethylene (PTFE or Teflon), has partially crystalline organization responsible for the morphological stability of the polymer. The main chain is linked at the side chains of perfluoro terminated with sulfonic acid group, which are responsible for the hydrophilic characteristics and thus the hydration and proton mobility within the membrane. (KREUER *et al*, 2004) (MAURITZ and MOORE, 2004) (JANNASCH, 2003).

According to Zhang (2008) the membrane is highly ion conductive because the SO_3 (Sulfonic Acid) extremity acts as a cation transporter, causing the membrane to conduct only protons and not electrons or anions. The fuel cells performance depends heavily on the ion exchange membrane hydration. The water transport through the membrane and maintaining a best condition of moisture is extremely important for the performance of a fuel cell (PIVOVAR, 2006). Adachi *et al* (2010) studied thickness dependence of water permeation through proton exchange membranes.

The authors discovered that water permeation rates did not increase linearly with decreasing thickness. Interfacial water transport resistance was found dominant for thinner

membranes. Majsztrik *et al* (2007) found that water sorption was limited by the rate of swelling of the Nafion®. The analysis of water permeation and sorption data made by the authors identified different regimes of water transport and sorption in Nafion® membranes corresponding to diffusion through the membrane, interfacial transport across the membrane–gas interface and swelling of the polymer to accommodate water. Studying the transport of liquid water through Nafion® membranes Duan *et al* (2012) found that liquid water is forced through hydrophilic domains in Nafion® by hydraulic permeation.

In addition the hydraulic permeation increases with hydrophilic volume fraction. Safronova *et al* (2015) investigated the mechanical properties of a perfluorosulfonic acid MF-4SC membrane (Russian analogue of Nafion®) in the H^+ and Na^+ ion forms at different of relative humidity (RH) values. The decrease in the Young's modulus at RH>32% was associated with the occurrence of weakly bonded water, which acts as a plasticizers.

The ion conductivity of the initial and broken membranes was investigated in different directions-parallel and perpendicular to the strain of the sample. The authors found a changing in conductivity and in anisotropy of the broken membranes caused by the reorganization of the system of pores and channels during strain, which differs by the water uptake of the samples. In this context, water management is very important for the fuel cell to achieve maximum power.

The nature of the water in the interdomain membrane structure is still a matter of debate and hence it is of paramount importance to find new methods to check the Nafion® membrane hydration, since the water content has influence in the ion transport performance within this polymer and this characteristic has direct consequences on PEM's efficiency.

In this work, measurements in terms of time in water were the main basis for a spectroscopic analysis of membrane hydration in the near and mid-infrared range. The Photoacoustic Spectroscopy (PAS) that is a non-destructive technique and allows spectroscopic analysis in the visible and infrared was used (DIAS, 2014; ROSENCWAIG, 1980).

The experiments were carried out in 200-2600 nm, since overtones of hydroxyl bonds and combinations thereof are easily defined or separated in this spectral region. It is expected that the absorption bands can provide information about the behavior of membrane hydration.

2. Photoacoustic Spectroscopy

Photoacoustic Spectroscopy is a method that allows obtaining optical absorption spectra of solid, semi solid, liquid and gas. It is a versatile technique that allows the analysis of samples optically opaque and transparent. Light scattered by the sample, which is a serious problem in other optical spectroscopic techniques, does not cause any significant problem for photoacoustic, since only the light that is absorbed by the sample is converted to the desired signal. This technique, in most cases, does not need a rigorous sample preparation. Another advantage is that being a non destructive technique allows the monitoration of the same sample when subjected to others chemical treatments, thermal, physical…

PAS is based on the photoacoustic effect (PA). The PA effect is obtained in a cell which comprises a closed container filled with a gas (usually air) where there is a glass window that allows the entry of light. A modulated light beam passes through the window, reaches the sample and it is absorbed. By a process of non-radiative deexcitation, the absorbed radiation is converted into thermal energy.

For the photoacoustic signal production in a solid sample, there are three basic mechanisms that coexist (BENTO *et al*, 2002): the thermal diffusion, the thermal expansion and the thermoelastic expansion.

In the first case, there is heat flow from the sample by the surrounding gas, causing in it a variation of temperature with the same modulation frequency of incident light. However, only a thin layer of gas in the sample vicinity, that responds to heat the sample temperature fluctuations. This layer will produce a cyclical process of expansion/contraction, functioning as a vibrating piston to the rest of the gas column, thereby generating the photoacoustic signal. This signal is detected by a microphone in a chamber connected to the photoacoustic cell. This explanation is also called the thermal piston model. (ROSENCWAIG and GERSHO, 1976*)*.

In the second case, the mechanical vibration, due to expansion and contraction of the sample itself, is coupled with the vibration of the thin layer of gas, acting on the rest of the column of gas as a piston (MACDONALD and WETSEL, 1978).

The third mechanism appears when the sample is trapped at their extremities. The light incident on the sample generates a temperature gradient inside, perpendicular to its larger side. Due to this gradient, the thermal expansion will be dependent on the depth, flexing the

sample. This periodic bending causes the sample surface produces photoacoustic signal (ROUSSET , LEPOUTRE and BERTRAND, 1983).

In other works, experimental setup for PAS is described (DIAS, 2014) (BENTO *et al*, 2002). The photoacoustic absorption spectra give important elements in the study of energy bands of a given element, since it allows the optical transitions assignment involved. Moreover, it can offer some information concerning the coordination state of a given ion housed in an array as well as its oxidation state (NAKAMURA, 1991). Employing the Phase-Resolved Photoacoustic Method (PRPA) (BENTO *et al*, 2002), we can characterize and distinguish between two (or more) absorbing centers present in the same matrix. The PPRA is a numerical method used in PAS (CESAR *et al*, 1984) to separate a spectrum when it is composed of more than one absorber center. For example, for the PA signals S_A (λ_1) and S_B (λ_2) with overlapping bands and centered on two nearby wavelengths ($\lambda_1 \approx \lambda_2$).

In principle, if the PA signals have a phase difference $\Delta\phi \neq 0$ in a wavelength chosen we may be able to resolve the spectra for each component. For the case we are analyzing in this paper, the lower limit of the phase difference is assumed a $\Delta\phi > 5^0$. In this method, the PA signal is represented in a phasor image, where it should be separated into two components, in phase and in quadrature, as shown in **Figure 1**. The contribution of the absorber center B is separated for a particular projection angle θ_B and it's maximum PA signal will be at $\theta_B \pm 90^0$.

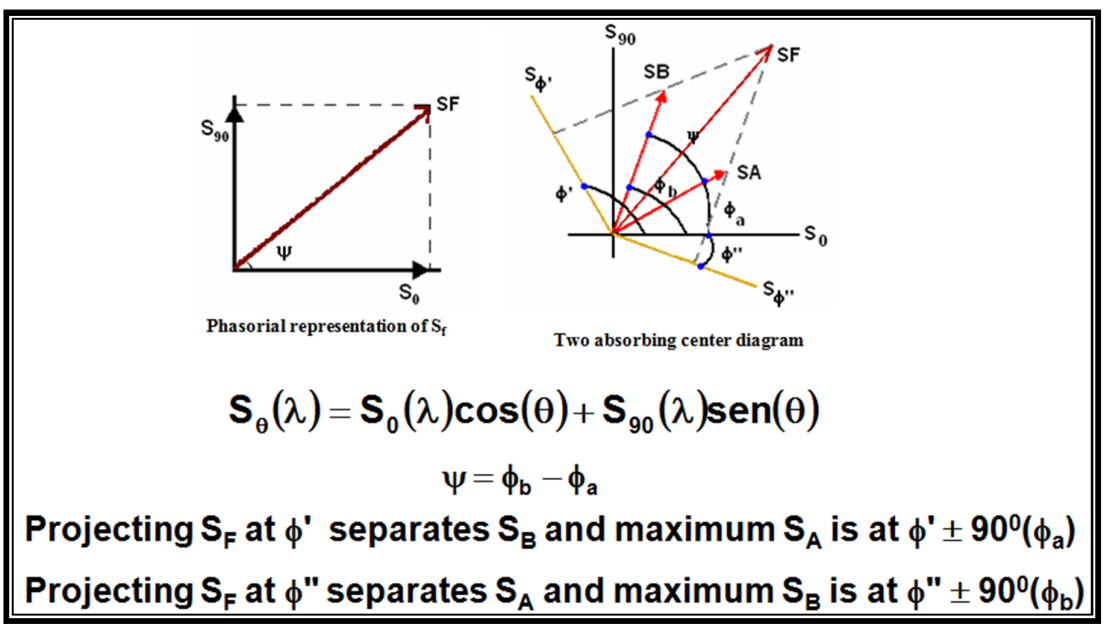

Figure 1: Phasorial diagram for PRPA
Source: Bento *et al* (2002).

3. The Membrane

The membrane used was Nafion® 117 (basis weight 360 g/m^2 and a thickness of 183 μm) in acid form (Nafion® -H) DuPont, provided by FuelCellsEtc (College Station, Texas). The general chemical structure can be seen in **Figure 2**, where a = 6.5, X is either sulfonic or carboxylic functional group and M is either a metal cation in the neutralized form or an H^+ in the acid form.

$$\begin{array}{l} [(CF_2CF_2)_a\text{—}(CFCF_2)]_b \\ \qquad\qquad\quad | \\ \qquad\qquad\quad O\text{—}CF_2\text{—}CF(CF_3)\text{—}O\text{—}CF_2CF_2\text{—}X^-M^+ \end{array}$$

Figure2: Perfluorinated ionomer Nafion®
Source: Dias *et al* (2005-a)

The PAS was used to check the OH bands. The procedure for the measurements was performed in essays as shown in **Table 1**, wherein: (I) Nafion® *in natura*; (II) placed in distilled water: 1 in 1 h up to 11 h and (III) 24 and 25 h in water after the start of the experiment.

For PRPA the procedure was different for each spectral region. In the near infrared (NIR) spectra were carried as the experimental essays (I) - (III). In the mid-infrared region (MIR) the membrane was placed in distilled water in the following essays: (i) 10 in 10 min up to 1:30 h after the start of the experiment, (ii) from 1:30 h was measured 1 in 1 h up to 11 h (iii) 24 and 25 h in water after the start of the experiment.

Table 1 – Experimental Essays

Photoacoustic Spectroscopy 200-2600 nm:	
Essay I	Nafion® *in natura*
Essay II	Placed in distilled water: 1 in 1 h up to 11 h
Essay III	24 and 25 h hydration
PRPA, 800-1600 nm: I, II and III essays only.	
PRPA, 1600-2600 nm: addition of the essay I,	
Essay i	placed in distilled water: 10 in 10 min up to 1:30 h
Essay ii	from 1:30 h was measured 1 in 1 h up to 11 h
Essay iii	24 and 25 h hydration.

Source: Author's Own

Importantly, the thickness of the sample increases with the time of immersion in water (DIAS *et al*, 2005-a). The initial thickness, measured by micrometer, *in natura* sample was ~198 μm, after that there was an apparent stabilization in the 2-6 h region (~207 μm) and finally saturated after 8 h (~209 μm). All experiments were performed at room temperature and about 50% relative humidity.

4. Results and discussions

4.1. Spectroscopy

Photoacoustic Spectroscopy was applied at 20 Hz modulation frequency, 800 W, and in three spectral regions: ultraviolet-visible (200-800 nm) in the near (800-1600 nm) and medium (1600-2600 nm). **Figure 3** shows the main absorption bands assigned to the Nafion® *in natura* (essay I, **Section 3**) in the ultraviolet-visible region [**Figure 3** (a)], NIR (**Figure 3 (b)**) and MIR (**Figure 3 (c)**). **Figure 3 (a)** shows two absorption bands at approximately 230 nm and 273 nm. The absorption at 230 nm is usually referred to as a diene structure (ALMEIDA and KAWANO, 1997).

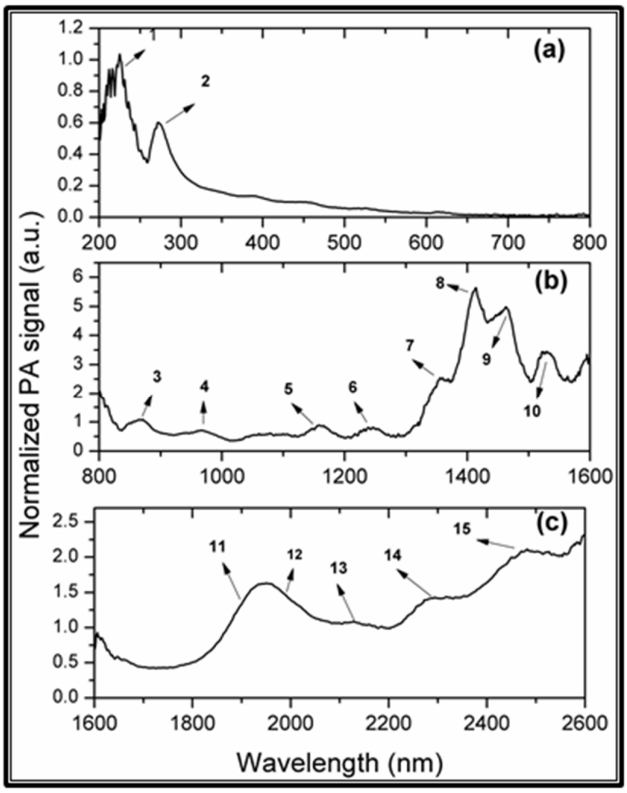

Figure 3: Nafion® *in natura* PA espectra: (a) UV-VIS (b) NIR and (c) MIR.
Source: Author's Own

The region between 800-2600 nm is dominated by the stretching modes and combinations O-H. **Figures 3 (b)** and **Figure 3 (c)** show about eight and five major bands absorption, respectively for the NIR and MIR. The PA signal is divided by a scale factor since it has arbitrary unit. For the absorption bands allocation, the peaks were listed and categorized as shown in **Table 2**, wherein overtones band refers to the harmonics of the bands which are repeated at certain frequencies. According to **Table 2** the monitoring of the hydration process will be conducted for evaluating the absorption bands peaks related to 9 and 11. These absorptions must correspond to OH stretching vibrations occurring SO_2-OH groups and hydroxyl groups involved in hydrogen bonds of different intensities formed between the sulfonic acid groups among the sulphonic acid molecules and water, and among the molecules of water. Furthermore, water molecules can bond to oxygen of the fluorinated ether side chains.

Table 2: Absorption bands for Nafion® sample.

Peak	Wavelength		Description
	nm	cm^{-1}	
1	230	43478	Diene structure
2	273	36630	Carbonyl group derived from radical group
2	200-300	50000-33333	CF_3He system $CF_2(^1B_1\text{-}^1A_1)$
3	878	11390	3° overtone ν(CH_2) **(1)**
4	988	10120	2° overtone ν(OH)
5	1189	8410	2° overtone ν(CH_2)
6	1250	8000	2° overtone characteristic -CH_2- and CH_3-group
7	1340	7460	Terminal methylene groups combination.
8	1400	7142	OH free, first overtone.
9	1450-1490	6896 - 6711	OH band, 1° overtone, superimposed to 3° overtone
10	1540	6495	1° overtone ν(OH)
11	1800-1920	5555-5208	OH free, combination
12	1932	5176	2° overtone ν(C=O)
13	2141	4670	ν(CO)+ ν(CH_2)
14	2240	4464	νch+ characteristic -CH_3 group combination
15	2466	4055	3° overtone δ(CC)

Source: Dias (2002); Almeida and Kawano (1997); Vagnini (2009); Suto (1983).

4.2. OH Absorption Band Monitoring

Monitoring of the polymer hydration and analysis of the OH bands at 1400 and 1850 nm was carried out as essays I (*in natura*), II (hydrous 1 in 1 h up to 11 h), and III (hydrate for

24 and 25 h) described in **Section 3**. **Figure 4** shows the absorption bands evolution for these experiments for the NIR region (**Figure 4 (a)** and **Figure 4 (b)**) and MIR (**Figure 4 (c)** and **Figure (d)**).

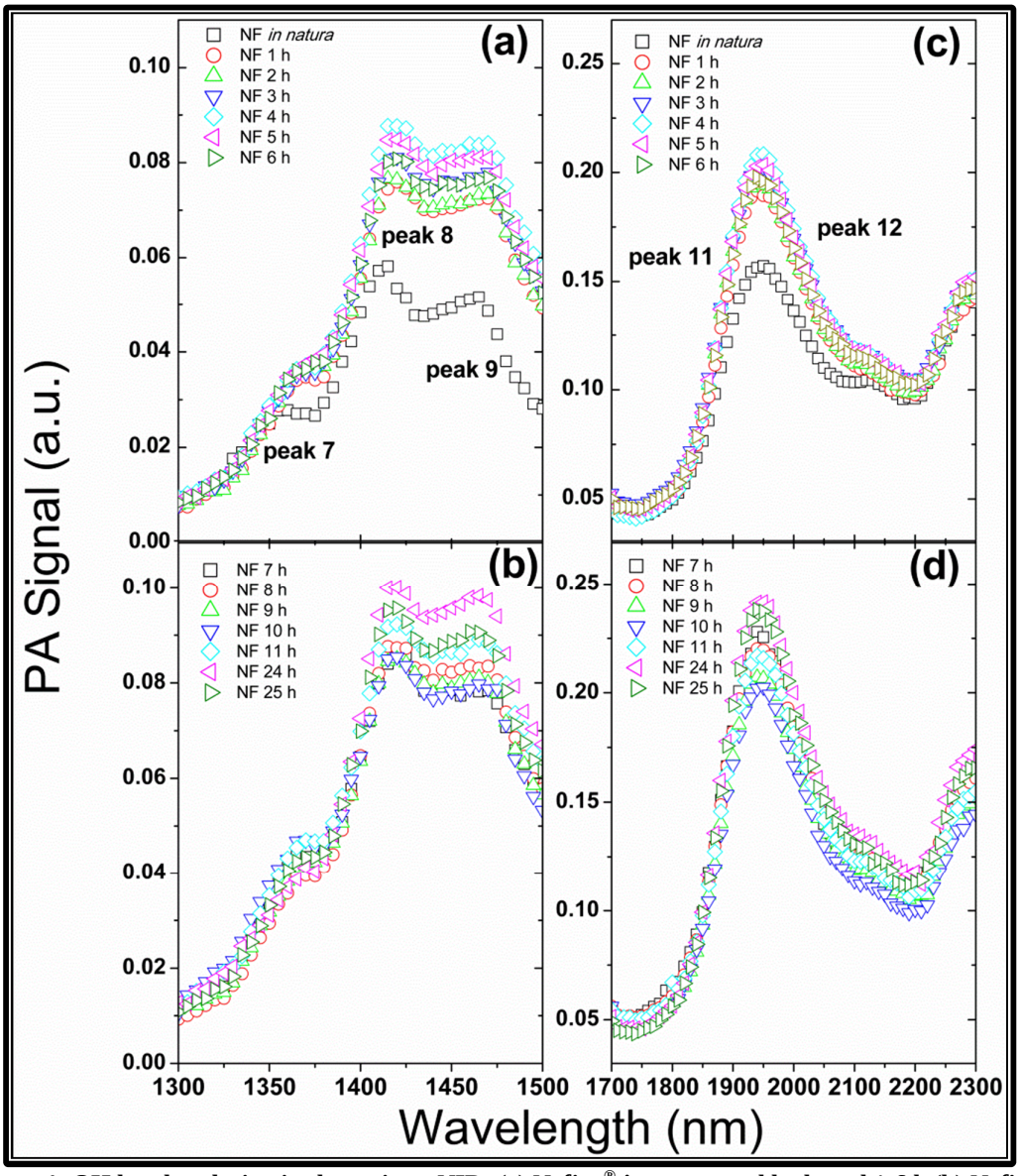

Figure 4: OH band evolution in the regions, NIR: (a) Nafion® *in natura* and hydrated 1-6 h (b) Nafion® hydrated 7-11 h, 24- 25 h and MIR: (c) Nafion® *in natura* and hydrated 1-6 h (d) Nafion® hydrated 7-11 h, 24- 25 h.
Source: Author's Own

For comparison, the spectra were normalized to start at the same photoacoustic signal. It can be observed in **Figures 4 (a)** and **Figure 4 (c)**, that in the first hour of hydration there is an increase in the photoacoustic signal between 1400-1475 (NIR) and 1850 to 2000 nm

(MIR). From an hour a little gradual increase occurs followed by an unexpected trend. Some experimental essays with high moisture content had lower photoacoustic signal. The **Figure 4 (b)** and **Figure 4 (d)** show that there isn't a significant increase in the photoacoustic signal for samples with high water content compared to the first time, these results proved one possible system saturation and reorganization of the clusters.

As shown in **Table 2** the absorption peaks are related to OH bands (peak 8, 9 and 11), to the terminal methylene groups (peak 7) and to ν(C=O) (peak 12). For a comparative analysis of the different intensities of the photoacoustic signal during the hydration of Nafion® it was applied a tool to do a depth profile of the sample. This tool, known as Phase-Resolved Photoacoustic Method was described in **Section 2** and the results are shown in **Section 4.3**.

The **C = O** stretching relating the peak 12 was found to be dependent on the degree of hydration of the membrane (see **Figures 4 (b)** and **Figure 4 (d)**). The band at 1932 nm may be associated to C = O groups located inside the side chain. Thus, C = O groups could be closer to ionic groups and would be subject to the effects of electrostatic field of the cation. This would explain the vibration dependence of these groups with the degree of membrane hydration.

4.3. PRPA

Due to the importance of analyzing and relating the changes in properties as a result of hydration of the Nafion® membrane the Phase-Resolved Photoacoustic Method was applied in the experimental essays I, II and III.

Figure 5 shows the spectra separation via PRPA, typically into the sample *in natura*. Each curve represents the total projected spectrum for the phase angle indicated. Using the PRPA, it was possible to separate the terminal methylene groups (peak 7 at 1340 nm) and the OH overtone (peak 9 at 1400 nm).

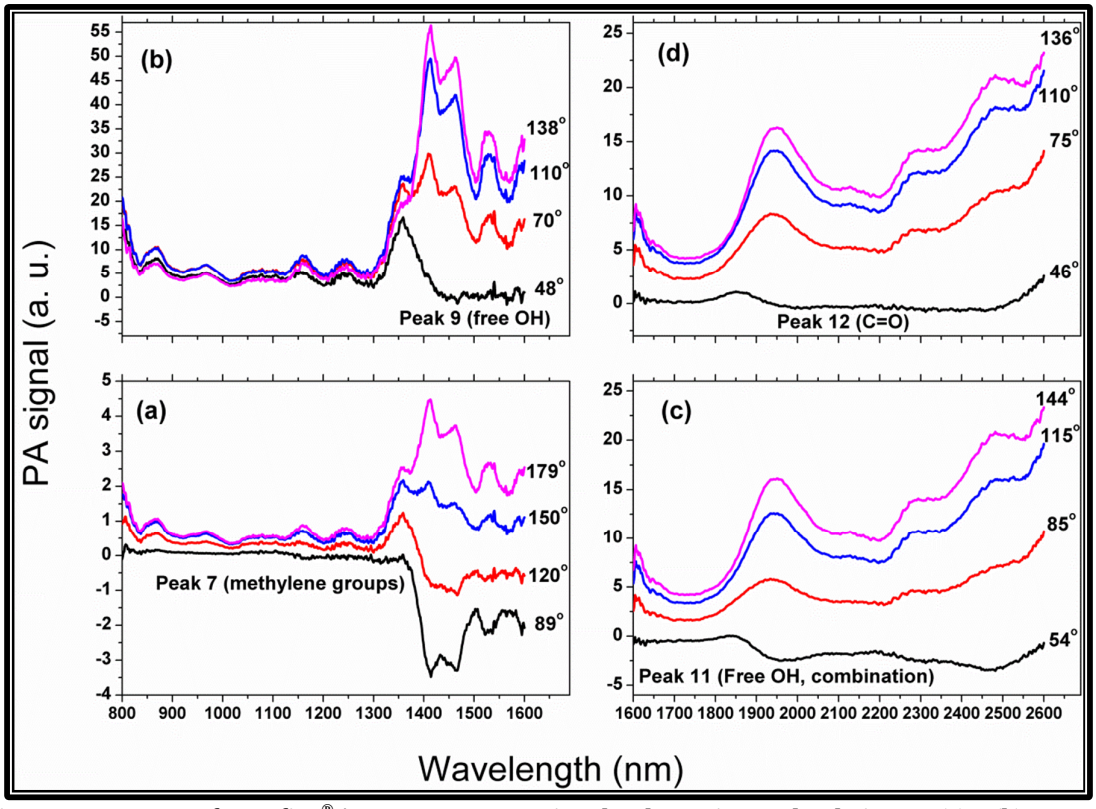

Figure 5: PA spectra for Nafion® *in natura*. NIR, zeroing the absorption peak relating to: (a) 7 (b) 9. MIR, zeroing the absorption peak relating to: (c) 11 (d) 12.
Source: Author's Own

In **Figure 5 (b)** is observed that the absorption band related to the peak 9 (at 1450 nm) decreases until it disappears completely around a phase angle of 48°. This means that the maximum absorption peak of the band occurs for a phase angle of 138°. Similarly it is observed in **Figure 5 (a)**, the peak 7 at 1350 nm disappears around 89° (ϕ_7= 179°). In the MIR spectrum at 1850 nm (peak 11) due to the free OH combination, has maximum absorption around 144°, as shown in **Figure 5 (c)**, and the peak 12 due to the C = O group at 1950 nm around 136°, see **Figure 5 (d)**. This is indicative of the existence of two absorbing centers with different times of relaxation.

The PA analysis showed no separation for the first and third overtone groups OH (peaks 8 and 9) as indicated in **Figure 6**. These bands had a maximum absorption around 95°, zeroing together at 5°, indicating that this region has only one relaxation time, i.e. absorbing centers are simultaneous. On the other hand, **Figure 6** presents the phase shift of ≈ 41° between peaks 7 and 9, for Nafion® *in natura*, before discussed.

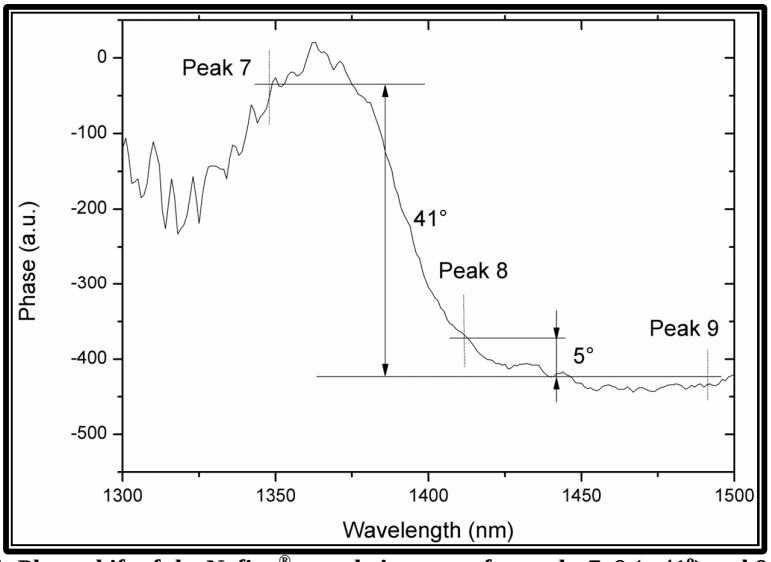

Figure 6: Phase shift of the Nafion® sample *in natura* for peaks 7, 9 (≈ 41º) and 8,9 (≈ 5º).
Source: Author's Own

The phase shift for Nafion® *in natura* is shown in the phasorial diagram, in **Figure 7 (a)**, for NIR, and in **Figure 7 (b)**, for MIR. The phases in which the spectra are separated (ϕ_i' and ϕ_j'') and the phase difference between the signals of absorbing groups (ψ) for all essays were found for the NIR and MIR. Recalling that $\psi_{i,j} = \theta_i - \theta_j$, for i = 7, and 11 (related to peaks 7 and 11) and j = 9 and 12 (peaks 9 and 12). The results for the phase difference were normalized with the respective values of the Nafion® *in natura*.

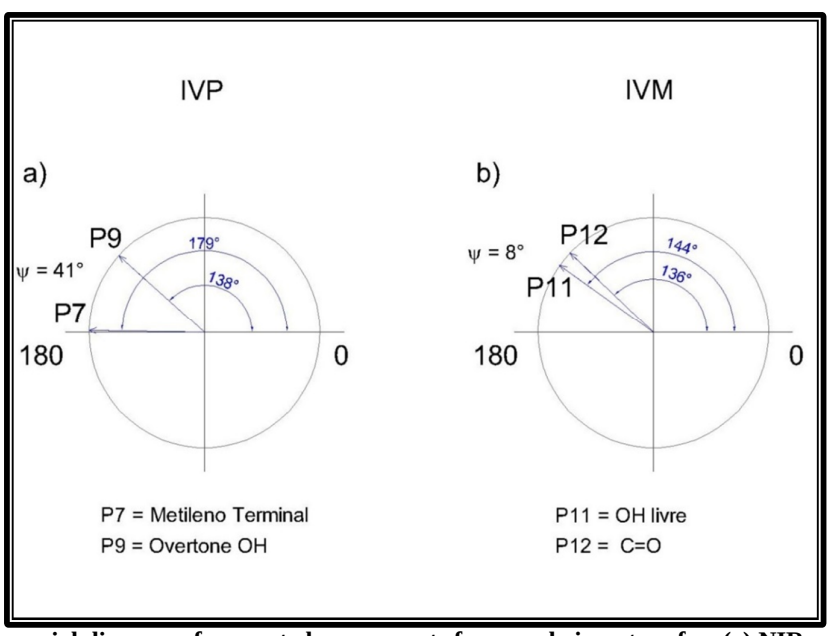

Figure 7: Phasorial diagram of separated components for sample *in natura* for: (a) NIR, and (b) MIR.
Source: Adapted from Bento *et al* (2002)

Figures 8 (a) and **Figure 8 (b)** show the tendency of the phase difference as a function of hydration time for the NIR ($\psi_{7,9}$) and MIR ($\psi_{11,12}$) regions respectively.

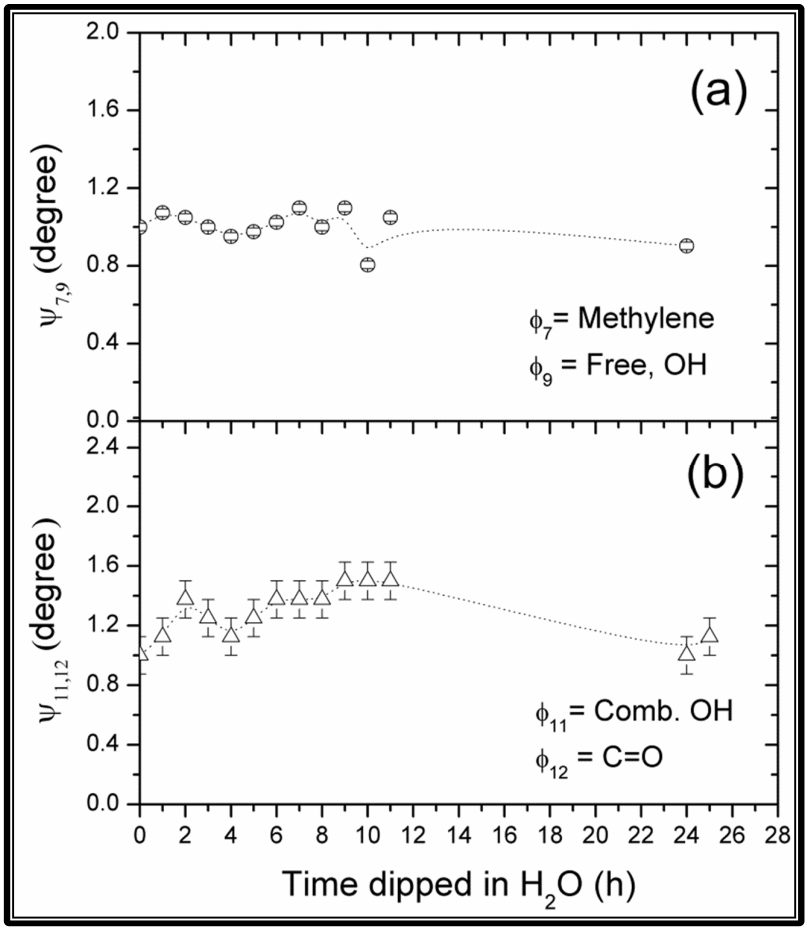

Figure 8: Comparison of the phase difference as a function of hydration time for essays (I), (II) and (III) in the regions: (a) NIR and (b) MIR.
Source: Author's Own

In **Figure 8 (a)** during the hydration the phase difference presented close values to the polymer *in natura* and was observed a maximum in 2 h ($\cong 0.9^0$) and in 9 h (1.1^0), possibly saturating after 24 h. For MIR, **Figure 8 (b)**, during hydration the phase difference was greater than the polymer in nature up to 24 hours, and observed a maximum in 2 h ($\cong 1.4^0$) and in 10 h ($\cong 1.5^0$). The values of $\psi_{7,9}$ were around four times higher than the $\psi_{11,12}$.

Dias *et al* (2005-a) measured the thermal diffusivity versus water content in the membrane and they found an opposite behavior compared to the tendency of the phase difference observed in the **Figure 8 (a)** and **Figure 8 (b)**. The thermal diffusivity behavior as a function of immersed time in water presented a minimum near 2 h ($\approx 3.00\times10^{-4}$ cm^2/s) and

11 h (5.00×10^{-4} cm^2/s). Possible saturation was also observed after 28 h (5.50×10^{-4} cm^2/s). After water uptaking, the thermal diffusivity is smaller than that for the polymer as received (6.54×10^{-4} cm^2/s). The authors explain that maybe the water occupies some Nafion® porous and, because of the high specific heat of water, the heat mighty be retained.

In the tendency of the **Figure 8,** in both cases ($\psi_{7,9}$ e $\psi_{11,12}$) a maximum phase difference is an increase in the OH absorption band, since the phase difference of the peaks in the NIR and MIR were evaluated in module $\Delta\varphi=|\phi_i-\phi_j|_{hydrous}-|\phi_i-\phi_j|_{in\ natura}=[(S_i/S_j)_{hydrous}]/(S_i/S_j)_{in\ natura}$ (DIAS *et al*, 2005-b). Therefore, this behavior approximately "mirrored" to the phase difference, when it's compared with the thermal diffusivity suggests that the hydration management governs the heat propagation.

When the membrane hydration increase possibly the thermal diffusivity will decrease and the inverse is also true. This effect is more visible to the MIR (**Figure 8 (b)**) than in the NIR (**Figure 8 (a)**). Possible because the band at 1400 nm is due to the free OH and in the 1850-1950 nm region is a OH groups combination that stay in the hydrophilic regions and may be attributed to OH groups that do not take part in hydrogen bonding and possibly would be exposed to the fluorocarbon. Probably are water molecules and hydroxyl that joined at the end of the secondary copolymer chain mainly at the edges of the internal micelles. In other words, the OH molecules can be trapped in clusters, depending on the type of the connections of Wan der Waals (LIU *et al*, 2013), formed between the oxygen sulfide terminal, and hydrogen from water (PERLES, 2008). Another hypothesis is that there was a change in its structure, or otherwise, a part of the water interacted with the structure and may have been the phenomenon known as water plasticizing (JUNG and KIM, 2012).

The hydrogen bonds formation decreases the electron density of orbital link O-H, weakening it. In higher wavelengths, hydroxyl that takes part in hydrogen bonds shows vibrations (compared to unrelated hydroxyl). This change will be greater when hydrogen bonds are stronger, due to the bigger weakening of the O-H bond. So absorptions around 1400 nm should match with the weaker hydrogen bonds, while absorptions around 1850-1950 nm can be attributed to stronger hydrogen bonds.

Therefore the thermal diffusivity is affected by an effects summation and constant reorganization of ion exchange. With the membrane hydration, there is a plasticizing effect of water (JUNG and KIM, 2012), it favors the chain segments mobility. The hydration also dramatically increases the diameter of the ion clusters, causing coalescence between them and

thus forming large ionic domains. Overall, the results revealed a great Photoacoustic Spectroscopy point of maximum thermal diffusivity close to saturation, i.e. around one hour of hydration, avoiding heating and facilitating the cooling of the membrane. These results were in agreement with other analyzes as a water content function made by the author (LOPES, 2016) in Thermogravimetric Analysis and Differential Scanning Calorimetry.

5. Conclusion

Photoacoustic spectroscopy allowed a non-destructive investigative analysis of the material, and monitoring their hydration. The membrane spectroscopic study indicated the different behaviors of the OH absorption bands that enabled the monitoring of hydration in Nafion®. The results showed a sudden increase of the PA signal in the early hours of hydration and possible saturation. The PRPA was able to separate the bands OH combinations of terminal methylene groups and C=O stretches. The behavior of the phase difference as a hydration time function predicts the results for the thermal diffusivity and the constant structural change, primarily related to the change in the number of ion clusters. In general, the findings showed that for best performance of the Nafion® membrane is optimum for the higher thermal diffusivity region and anterior to saturation (1 h).

6. References

ADACHI, M. *et al*, Thickness dependence of water permeation through proton exchange membranes, **Journal of Membrane Science**, v. 364, p. 183-193, 2010.

ALMEIDA, S. H.; KAWANO, Y. Ultra Violet – Visible Spectra os Nafion Membran, **European Polymers Journal**, v. 33, n. 8, p. 1307-1311, 1997.

BENTO, A. C. *et al*, On the Application of the Photoacoustic Methods for the Determination of Thermo-Optical Properties of Polymers, **Brazilian Journal of Physics**, v. 32, n.2B, p. 483-494, 2002.

CESAR, C.L. *et al*, Phase-resolved photoacoustic microscopy: Application to ferromagnetic layered samples, **Journal of Applied Physics**, v. 55, p. 3460-3464, 1984.

CHURCH, S. Del. Firm installs Fuel cell, **The News Journal**, v. 2, p. B7, 2006.

DIAS, D. T. Análise de defeitos residuais em papel comercial através de Espectroscopia Fotoacústica. **Revista Brasileira de Física Tecnológica Aplicada**, v. 1, n. 2, p. 1-9, 2014.

DIAS, D. T. *et al*, Open Photoacoustic Cell study of thermal diffusivity of Nafion® as a function of water content. **Journal de Physique IV**, v. 125, p. 383-386, 2005-a.

DIAS, D. T. *et al*, Statistical design of experiments: study of cross-linking process trough phase-resolved photoacoustic method as multivariable response. **Applied Spectroscopy**, v. 59, n. 2, p. 173-180, 2005-b.

DIAS, D. T. *et al*, Photoacoustic study of cross-linking process in grafted polymer and copolymer based on ethylene and vinyltrimethoxy silane. **Journal of Physics D: Applied Physics**, v. 35, p. 3240-3248, 2002.

DUAN, Q. *et al*, Transport of liquid water through Nafion membranes, **Journal of Membrane Science**, v. 392-293, p.88-94, 2012.

JANNASCH, P. Recent Developments in high-temperature proton conducting polymer electrolyte membranes. **Current Opinion in Colloid & Interface Science**, v.8, p. 96-102, 2003.

JUNG, H. and KIM. J. W. Role of the glass transition temperature of Nafion 117 membrane in the preparation of the membrane electrode assembly in a direct methanol fuel cell (DMFC). **International Journal of Hydrogen Energy**, v. 37, p. 12580-12585, 2012.

KREUER, K. D. *et al*, Transport in Proton Conductors for Fuel-Cell Applications: Simulations, Elementary Reactions, and Phenomenology. **Chemical Reviews**, v. 104, p. 4637-4678, 2004.

LIU, S., *et al.* Water - Ionomer Interfacial Interactions, Investigated by Infrared Spectroscopy and Computational Methods. **Lagmuir**, v. 29, n. 45, p. 13890-13897, 2013.

LOPES, G. **Caracterização de membrana nafion usando espectroscopia fotoacústica: monitoramento da hidratação**. Dissertação de Mestrado, UTFPR, Ponta Grossa, 2016.

MACDONALD, F. A.; WETSEL G. C. Generalized theory of the photoacoustic effect, **Journal of Applied Physics**, v. 49, p. 2313-2322, 1978.

MAJSZTRIK, P. W. *et al.*, Water sorption, desorption and transport in Nafion membranes, **Journal of Membrane Science**, v. 301, p. 93-106, 2007.

MAURITZ, K. A.; MOORE, R. B. State of Understanding of Nafion**. Chemical Reviews**, v. 104, p.4535-4585, 2004.

NAKAMURA, O. **Aplicações da Espectroscopia Fotoacústica e Ressonância Paramagnética Eletrônica ao Estudo de materiais Catalíticos**, Tese de Doutorado, UNICAMP, Campinas, SP, 1991.

PERLES, C. E. Propriedades físico-químicas relacionadas ao desenvolvimento de membranas de Nafion® para aplicações em células a combustível do tipo PEMFC, **Polímeros: Ciência e Tecnologia**, v. 18, n. 4, p. 281-288, 2008.

PIVOVAR, B. S. An Overview of electro-osmosis in fuel cell polymer electrolytes, **Polymers,** v. 47, n. 11, p.4194-4202, 2006.

ROSENCWAIG, A. **Photoacoustic and Photoacoustic Spectroscopy**. New York: John Wiley & Sons, 1980.

ROSENCWAIG, A.; GERSHO, A. Theory of the photoacoustic effect with solids. **Journal of Applied Physics**, v. 47, p.64, 1976.

ROUSSET, G.; LEPOUTRE, F.; BERTRAND, L. Influence of thermoelastic bending on photoacoustic experiments related to measurements of thermal diffusivity of metals. **Journal of Applied Physics**, v. 54, p. 2383-2391, 1983.

SAFRONOVA, E. *et al*, Mechanical properties and influence of straining on ion conductivity of perfluorosulfonic acid Nafion®-type membranes depending on water uptake. **Journal of Membrane Science**, v. 473, p. 218-225, 2015.

SUTO, M.; WASHIDA, N. Emission Spectra of CF3 Radicals I. UV and Visible Emission Spectra of CF_3 Observed in the VUV Photolysis and the Metastable Argon Atom Reaction of CF_3H. **The Journal of Chemical Physics,** v. 78, p. 1007-1011, 1983.

VAGNINI, M. *et al*, FT-NIR Spectroscopy for Non-Invasive Identification of Natural Polymers and Resins in Easel Painting. **Analytical and Bioanalytical Chemistry,** v. 395, n. 7, p. 2107-2118, 2009.

ZHANG, J. **PEM Fuel Cell Electrocatalysts and Catalyst Layers.** Vancouver, BC, Canada: Springer, 2008.

7. Acknowledgment

The authors thank CAPES and CNPq for financial support.

8. Author's additional information:

Daniele Toniolo Dias: PhD in Physics, Academic Department of Physics, Federal University of Technology – Paraná, e-mail: danieletdias@utfpr.edu.br

Caroline Dias Rosa: Biology Student, Ponta Grossa State University, e-mail: carolinedias_rosa@hotmail.com

Juliana Soares de Souza: Mechanical Engineering student, Federal University of Technology – Paraná, e-mail: julianasdesouza@gmail.com

……

Artigo recebido para avaliação em 21/02/2016 e aceito para publicação em 27/05/2016.